

Article

Removal of Crotamiton from Reverse Osmosis Concentrate by a TiO₂/Zeolite Composite Sheet

Qun Xiang ¹, Shuji Fukahori ², Naoyuki Yamashita ³, Hiroaki Tanaka ³ and Taku Fujiwara ^{4,*}

¹ The United Graduate School of Agricultural Sciences, Ehime University, 3-5-7 Tarumi, Matsuyama, Ehime 790-8566, Japan; s16dre09@s.kochi-u.ac.jp

² Paper Industry Innovation Center of Ehime University, 127 Mendoricho Otsu, Shikokuchuo, Ehime 799-0113, Japan; fukahori.shuji.mj@ehime-u.ac.jp

³ Research Center for Environmental Quality Management, Kyoto University, 1-2 Yumihama, Otsu, Shiga 520-0811, Japan; yamashita@biwa.eqc.kyoto-u.ac.jp (N.Y.); htanaka@biwa.eqc.kyoto-u.ac.jp (H.T.)

⁴ Research and Education Faculty, National Sciences Cluster, Agriculture Unit, Kochi University, 200 Monobe Otsu, Nankoku, Kochi 783-8502, Japan

* Correspondence: fujiwarat@kochi-u.ac.jp; Tel.: +81-88-864-5163

Received: 29 June 2017; Accepted: 24 July 2017; Published: 31 July 2017

Abstract: Reverse osmosis (RO) concentrate from wastewater reuse facilities contains concentrated emerging pollutants, such as pharmaceuticals. In this research, a paper-like composite sheet consisting of titanium dioxide (TiO₂) and zeolite was synthesized, and removal of the antipruritic agent crotamiton from RO concentrate was studied using the TiO₂/zeolite composite sheet. The RO concentrate was obtained from a pilot-scale municipal secondary effluent reclamation plant. Effective immobilization of the two powders in the sheet made it easy to handle and to separate the photocatalyst and adsorbent from purified water. The TiO₂/zeolite composite sheet showed excellent performance for crotamiton adsorption without obvious inhibition by other components in the RO concentrate. With ultraviolet irradiation, crotamiton was simultaneously removed through adsorption and photocatalysis. The photocatalytic decomposition of crotamiton in the RO concentrate was significantly inhibited by the water matrix at high initial crotamiton concentrations, whereas rapid decomposition was achieved at low initial crotamiton concentrations. The major degradation intermediates were also adsorbed by the composite sheet. This result provides a promising method of mitigating secondary pollution caused by the harmful intermediates produced during advanced oxidation processes. The cyclic use of the HSZ-385/P25 composite sheet indicated the feasibility of continuously removing crotamiton from RO concentrate.

Keywords: paper-like composite sheet; zeolite; photocatalysis; reverse osmosis concentrate; pharmaceutical; inhibitory effect; intermediate

1. Introduction

Reverse osmosis (RO) is a well-established technology for water desalination, the production of potable water, and more recently, tertiary wastewater treatment [1,2]. With increasing global water demand, it is predicted that the global market value of RO system components will reach 8.1 billion USD by 2018 [3]. Along with the purification of wastewater, the RO process produces a concentrate containing high levels of rejected pollutants (about 15–20% of the influent volume) [4]. Some of the emerging pollutants, such as pharmaceuticals and personal care products, are very persistent in sewage effluent, resulting in raised awareness of the environmental risk of RO concentrates [1,5,6]. Genotoxicity evaluation using the *SOS/umu* test has provided direct evidence that RO concentrates have much higher toxicological risk than RO influents [7]. Therefore, suitable technology needs to be

developed for treating RO concentrates before discharging them into receiving water or recycling for other purposes. This requirement is especially important for large-scale RO treatment systems [8].

In a number of recent studies, TiO₂ photocatalysis has been used to treat pharmaceuticals in wastewater [9]. The nonselective oxidation ability of hydroxyl radicals enables effective degradation of various organic pollutants. However, the photocatalysis of target compounds can be inhibited by coexisting materials, such as inorganic ions and organic matter, in the wastewater [10–12]. In addition, toxic intermediates may be produced during photocatalysis, and the effects of pharmaceutical degradation products in the environment are of concern. Furthermore, when TiO₂ or nano-TiO₂ powder in water is exposed to ultraviolet (UV) radiation, radicals that are harmful to aquatic organisms are produced [13]. Therefore, the effective recovery of catalyst powder after wastewater treatment should be taken into consideration.

Wastewater treatment frequently involves adsorption processes, and various types of adsorbents have been developed to remove different pollutants [14–19]. The high-silica Y-type zeolite HSZ-385, which is a hydrophobic zeolite, has been used to remove sulfonamide antibiotics from wastewater and selectively removes sulfonamides even in the presence of high concentrations of coexisting materials [20]. However, after adsorption, the contaminants are permanently transferred to the sorbent and not destroyed, which can lead to problems with saturation of the adsorbent.

Attempts have been made to synthesize TiO₂-adsorbent composites that perform both photocatalysis and adsorption to remove pharmaceuticals from wastewater [21–23]. This synergistic effect has been confirmed for TiO₂ and zeolite in a TiO₂/zeolite composite powder that was used to remove sulfonamide antibiotics [23]. Wu et al. condensed nano-TiO₂ on the surfaces of carbon spheres through hydrothermal treatment to generate core-shell structures, and found that visible light absorption was enhanced compared with pure TiO₂ because of the interface formed between the two materials [21]. The activated carbon fiber felt (ACFF) in the TiO₂/ACFF porous composites significantly enhances the photocatalytic property of toluene by hindering the recombination of electron-hole pairs, reducing the TiO₂ band gap energy, and accelerating toluene adsorption [24]. Using a papermaking technique, Fukahori et al., prepared a paper-like composite sheet from TiO₂ and zeolite powder [25]. Under UV irradiation, bisphenol A was effectively degraded through the synergistic effect of the TiO₂ photocatalyst and zeolite adsorbent in these sheets [25]. In addition, the degradation intermediates of bisphenol A, which may be harmful to the environment, were temporarily captured by zeolite in the composite sheet and eventually decomposed through photocatalysis [26]. However, these studies were conducted using ultrapure water as the solvent, and the inhibitory effects of other components of the wastewater matrix have not been investigated.

In this study, we synthesized a TiO₂/zeolite composite sheet to remove of crotamiton from RO concentrate, and to recover the catalyst and adsorbent after water treatment. Crotamiton is a scabicide and antipruritic agent that has frequently been detected in sewage effluent in Japan because of its stable nature and wide consumption [27–29]. The effect of coexisting matter from the wastewater matrix on inhibiting crotamiton degradation was evaluated. In addition, the behavior of crotamiton degradation intermediates during photocatalysis was investigated.

2. Materials and Methods

2.1. Materials

HSZ-385 (surface area 600 m²/g, mean particle size 4 μm, SiO₂/Al₂O₃ ratio 100:1) was purchased from Tosoh Ltd. (Tokyo, Japan). TiO₂ powder (P-25, 50 m²/g, anatase) was purchased from Degussa (Dusseldorf, Germany) and F-type zeolite powder (F9, SiO₂/Al₂O₃ ratio 2.1:1) was purchased from Wako Pure Chemical Industries, Ltd. (Tokyo, Japan). Crotamiton (purity > 97%) and isotope-labelled surrogate crotamiton-d7 (purity 94.5%) were purchased from Sigma-Aldrich (St Louis, MO, USA) and Hayashi Pure Chemical (Osaka, Japan), respectively. Crotamiton-d7 was dissolved in methanol

(purity > 99.8%; Kanto Chemical Co., Inc., Tokyo, Japan) to prepare an internal standard solution, which was stored at $-20\text{ }^{\circ}\text{C}$. All other chemicals used were of reagent grade.

Composite sheets consisting of TiO_2 and zeolite (HSZ-385 or F-9) were prepared using a papermaking technique. TiO_2 , zeolite (3.125 g each), and polyethylene terephthalate fiber (6.25 g) were suspended in water (1 L); a cationic flocculant [poly-(amideamine) epichlorohydrin, 0.05% of total solid] and an anionic flocculant (anionic polyacrylamide, 0.084% of total solid) were sequentially added and the final suspension was stirred. Hand sheets with a grammage of 200 g/m^2 were prepared according to JIS P8222 [30]. The sheets were dried at $120\text{ }^{\circ}\text{C}$. The mass ratio of TiO_2 to zeolite in the composite sheet was 1:1. The TiO_2 /zeolite composite sheet used in this study contained 4 mg/cm^2 of TiO_2 and zeolite. Characterization of the TiO_2 /zeolite composite sheet was performed by scanning electron microscopy-energy dispersive X-ray spectroscopy (SEM-EDS: ProX; Phenom World) as shown in Figure 1. The SEM and EDS images revealed the uniform distribution of TiO_2 and zeolite powder in the composite sheet.

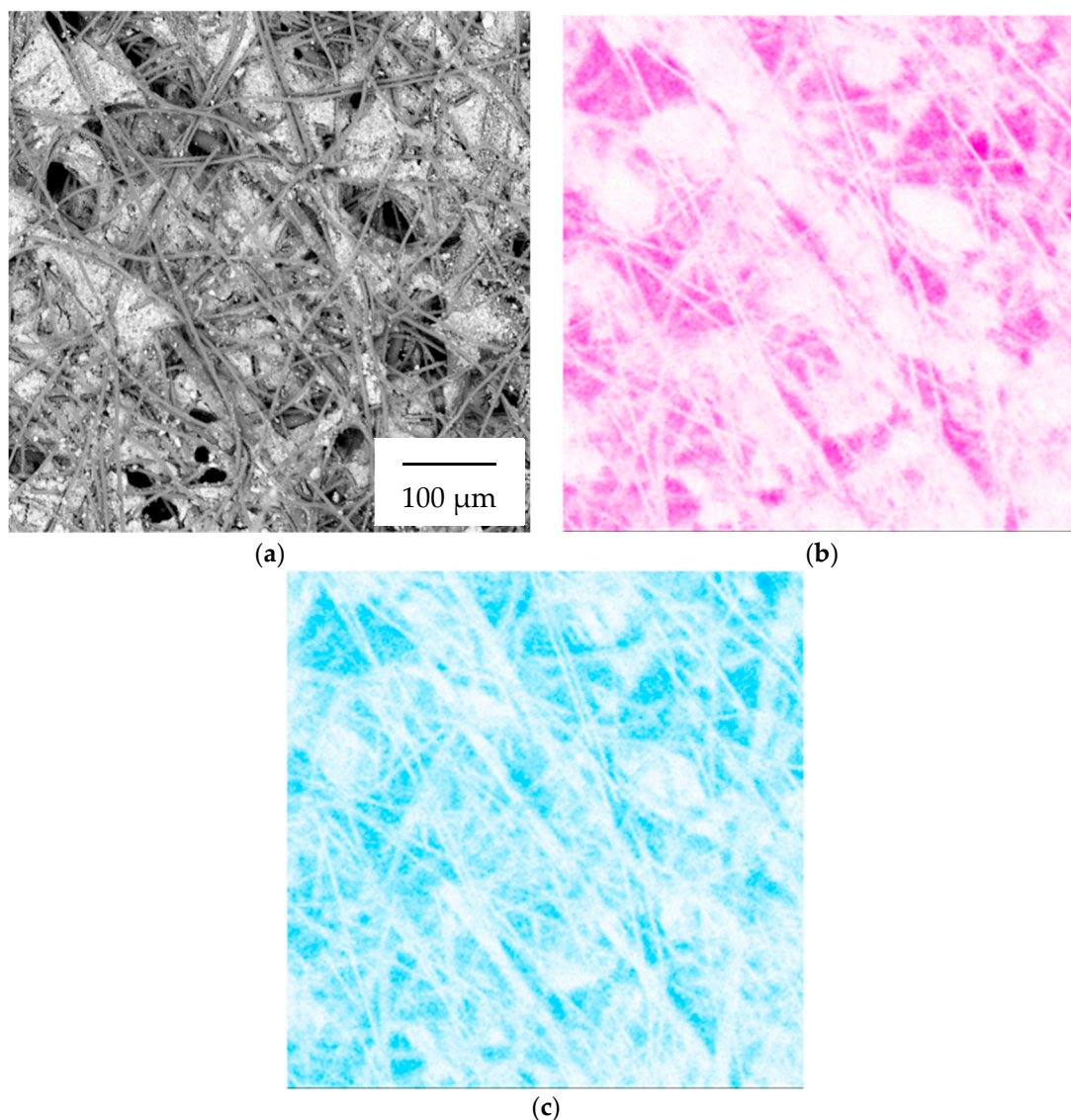


Figure 1. Scanning electron microscopy-energy dispersive X-ray spectroscopy (SEM-EDS) mapping images of TiO_2 /zeolite composite sheet: SEM images (a); EDS mapping of Si (b) and Ti (c).

RO concentrate was collected from a nanofiltration/RO pilot-scale plant for municipal secondary effluent reclamation on 7 March 2017 in Japan, and stored at 4 °C. The RO concentrate was analyzed and the results are as shown in Table 1. Details of the quantitative analyses are given in the Supplementary materials. To clarify the mechanism for removing of crotamiton with the composite sheet, crotamiton solutions were prepared using either RO concentrate or ultrapure water (Millipore, Tokyo, Japan).

Table 1. Water quality analysis of the reverse osmosis concentrate.

Parameter	Value	Ion	mg/L
pH	7.8	Na ⁺	223
Conductivity (mS/m)	170	NH ₄ ⁺	25.7
		K ⁺	26.4
TOC (mgC/L) ^a	10.1	Mg ²⁺	22.2
		Ca ²⁺	45.5
COD _{cr} (mg/L) ^b	22	Cl ⁻	316
		NO ₂ ⁻	15.6
UV absorbance (λ = 365 nm) (1/cm) ^c	0.049	NO ₃ ⁻	46.8
		SO ₄ ²⁻	87.5

^a TOC, total organic carbon; ^b COD_{cr}, chemical oxygen demand; ^c UV, ultraviolet.

2.2. Quantitative Analyses

To determine the concentration of crotamiton in the RO concentrate solution, solid phase extraction (SPE) was carried out. The cartridges (Oasis HLB, 60 mg, 3 mL, Waters, Milford, MA, USA) were conditioned with 2 mL of methanol, followed by 2 mL of ultrapure water. Aqueous samples spiked with the internal standard solution were then loaded onto the cartridges. Next, the cartridges were washed with 2 mL of ultrapure water and dried with a GL-SPE vacuum manifold system (GL Science, Tokyo, Japan) for 30 min. The analyte was eluted first with 1 mL of 10% methanol and then with 4 mL of methanol. The average recovery rate of crotamiton was 97 ± 1.7% (mean ± standard deviation, *n* = 3).

The concentrations of crotamiton were determined with the internal standard addition method using liquid chromatography tandem mass spectrometry (LC/MS/MS, Acquity UPLC-Xevo TQ; Waters) after SPE. The intermediates were identified from the mass spectral patterns obtained by LC/MS/MS.

2.3. Methods

Adsorption experiments were carried out by submerging the TiO₂/zeolite composite sheets (2 × 5.5 cm²) at a depth of 4 cm in 50 mL of the crotamiton solution (10 mg/L or 120 µg/L) at pH 7.0 ± 0.1 without ultraviolet irradiation (Figure S1). The mixture was stirred at a moderate speed at 25 °C. After a set treatment time, the treated solutions were passed through a DISMIC-13HP 0.2-µm membrane filter (Toyo Roshi Kaisha, Tokyo, Japan) to determine the crotamiton concentrations in the aqueous phase (*C_t*).

For the adsorption and photocatalytic degradation experiments, UV irradiation was applied perpendicular to the sheet surface (Figure S1) with a FL287-BL365 UV lamp (Raytronics, Tokyo, Japan), which had a maximum output wavelength of 365 nm. The UV intensity at the center of the reactor was controlled at 1000 µW/cm² using a UV-340C light meter (Custom, Tokyo, Japan). The other experimental conditions were the same as for the adsorption experiment. After a set irradiation time, the treated solutions were passed through 0.2-µm membrane filters, and the crotamiton concentrations (*C_t*) were then determined.

To measure the mass of crotamiton in the sheet, the composite sheet was soaked in methanol (purity > 99.8%). After ultrasonication for 60 min (38 kHz, 120 W; US-3KS; SND Co., Ltd., Nagano, Japan), the treated solutions were filtered through 0.2-µm membrane filters and analyzed by

LC/MS/MS (C_t'). The recovery rate for desorption was $107 \pm 1\%$. The mass of crotamiton in the treated solution ($M_{in\ water}$) was calculated using Equation (1), in which V is the solution volume.

$$M_{in\ water} = C_t \times V \quad (1)$$

Similarly, the mass of crotamiton in the composite sheet ($M_{in\ sheet}$) was calculated using Equation (2).

$$M_{in\ sheet} = C_t' \times V \quad (2)$$

The total mass of crotamiton remaining in the system ($M_{in\ system}$) was calculated using Equation (3).

$$M_{in\ sheet} = C_t' \times V \quad (3)$$

3. Results and Discussion

3.1. Adsorption of Crotamiton by the HSZ-385/P25 Composite Sheet

The HSZ-385/P25 composite sheet was applied to the adsorption of crotamiton in the RO concentrate. In preliminary experiments, we confirmed that crotamiton was rapidly adsorbed by HSZ-385 zeolite powder (Figure S2). We also confirmed that crotamiton was not adsorbed by P25 [31]. The crotamiton concentrations were plotted against time (Figure 2). Similar performances of the sheet in RO concentrate and ultrapure water revealed that other components in the RO concentrate (Table 1) did not obviously affect the adsorption of crotamiton by the composite sheet within the 24-hr treatment period.

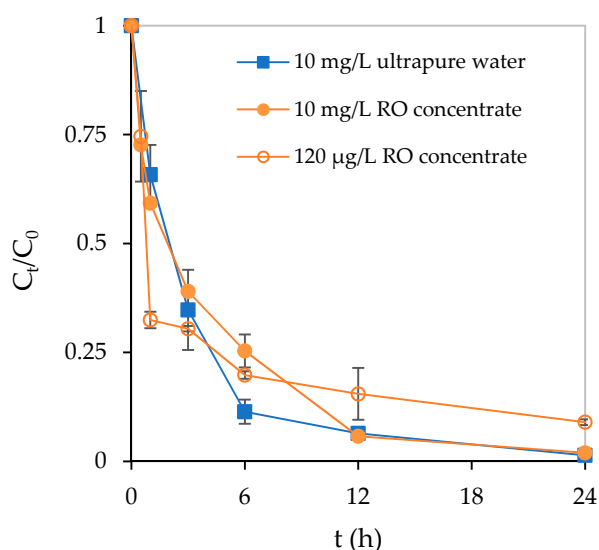


Figure 2. Adsorption of crotamiton using the HSZ-385/P25 composite sheet. Results are means \pm standard deviations ($n = 2$).

It has been reported that inorganic ions and organic materials affect the adsorption of pharmaceuticals [32]. Nevertheless, the adsorption of sulfonamide antibiotics from livestock urine and bisphenol A from landfill leachate by HSZ-385 was not affected by coexisting ions [14,20]. Meanwhile, even if the organic carbon content of porcine urine was two orders of magnitude higher than those of the sulfonamides, the sulfonamides were also effectively removed [20]. For bisphenol A, the removal efficiency decreased slightly when more than 50 mg/L humic acid was added [14]. Umar et al., reported that humic-like and fulvic acid-like matter in the RO concentrate were the major contributors to the color of the concentrate [33]. The RO concentrate used in this research appeared to be light brown. In the present study, when the HSZ-385/P25 composite sheet was used to adsorb the raw RO

concentrate without crotamiton spiking, only approximately 10% of the total organic carbon (TOC) was removed. Therefore, in the RO concentrate, crotamiton would be removed by adsorption on the composite sheet prior to the raw organic matter. In addition, the removal results for different initial crotamiton concentrations in the RO concentrate were similar, which implies that crotamiton can be adsorbed by the HSZ-385/P25 composite sheet over a wide range of initial concentrations.

We previously investigated the mechanism involved in the adsorption of sulfonamides to HSZ-385. We found that HSZ-385 adsorbed neutral sulfonamides more effectively than non-neutral sulfonamides, and that hydrophobic interactions played important roles in the adsorption process [34]. Crotamiton is hydrophobic ($\log K_{OW} = 2.73$) and has no ionizable functional groups. Therefore, hydrophobic interactions may play an important role in the adsorption of crotamiton by the HSZ-385/P25 composite sheet.

3.2. Photocatalytic Degradation of Crotamiton by the F9/P25 Composite Sheet

To clarify the photocatalysis of crotamiton by the F9/P25 composite sheet, the composite sheet was synthesized to be similar to the HSZ-385 composite sheet. Both F9 zeolite and the F9/P25 composite sheet did not remove crotamiton by adsorption (Figure S2). The F9 zeolite is a hydrophilic zeolite, whereas the Y-type zeolite HSZ-385 is a hydrophobic zeolite. This is further evidence that crotamiton is removed by HSZ-385 mainly through hydrophobic interactions.

The photocatalytic degradation of crotamiton over time by the F9/P25 composite sheet is shown in Figure 3. Direct photolysis of crotamiton was not observed [31]. The removal efficiency of crotamiton from the RO concentrate was much lower than that from the ultrapure water. After 24 hr of UV irradiation, the majority of the crotamiton in the ultrapure water was degraded. In contrast, ca. 50% of the crotamiton was degraded in the RO concentrate. Linear relationships were found between $\ln(C_t/C_0)$ and UV irradiation time (t) (Figure 3). Therefore, the first-order kinetic model shown in Equation (4) was used to evaluate the photocatalysis of crotamiton. In that equation, k_1 is the pseudo-first-order rate constant. The k_1 value for crotamiton removal from the RO concentrate by the F9/P25 composite sheet was 0.048 hr^{-1} , and was only half of that in the ultrapure water (0.092 hr^{-1}). Obviously, the lower rate constant reflects the effect of other components in the RO concentrate on the photocatalytic degradation of crotamiton.

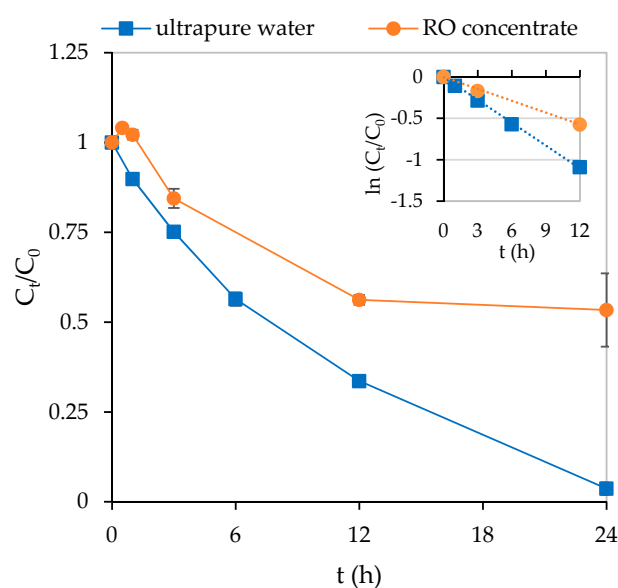


Figure 3. Photocatalytic degradation of crotamiton using the F9/P25 composite sheet with ultraviolet irradiation ($C_0 = 10 \text{ mg/L}$). The inset shows the fitting results of the first-order kinetic model. Results are means \pm standard deviations ($n = 2$).

$$\ln (C_t / C_0) = -k_1 t \quad (4)$$

UV absorbance is an important parameter affecting photocatalysis [10,35]. The maximum output wavelength of the UV lamp in our study was 365 nm, and the RO concentrate had an absorbance of 0.049 cm^{-1} at 365 nm (Table 1). Based on the Beer-Lambert law and the distance from the reactor surface to the sheet, the light transmittance was 82.1%. Therefore, after passing through the RO concentrate in the batch reactor, the light intensity at the sheet surface decreased by 17.9%, which is called the screening effect [36]. This effect contributed to the decrease in the photocatalytic degradation efficiency. Furthermore, the RO concentrate was light brown, and the color of the composite sheet surface changed from white to light brown after treatment of the RO concentrate. This color change could be caused by adsorption of coexisting materials on the sheet surface, and this could negatively affect the performance of TiO_2 photocatalysis through occupation of the active sites on the surface of TiO_2 [37].

The TiO_2 photocatalysis could be inhibited via the scavenger effect by coexisting ions [10,38–40]. The ions Cl^- and HCO_3^- have been found to inhibit photocatalysis through the hydroxyl radical and valence band hole scavenging [10,40]. Rioja et al., reported a marked deactivation effect caused by added salts for two tested acidic drugs [41]. Furthermore, Tokumura et al., suggested that coexisting matter could mitigate the generation of hydroxyl radicals through direct reactions with holes in the valence band and electrons in the conduction band of the photocatalyst [37]. As reported by Song et al., Cl^- can cause agglomeration of TiO_2 particles in a slurry by suppressing the stabilizing effect of electrostatic repulsion, reducing the effective contact surface between the photocatalyst and the pollutants [42]. In this research, the TiO_2 /zeolite composite sheet was used instead of TiO_2 powder. Therefore, even if the RO concentrate contained 316 mg/L Cl^- (Table 1), agglomeration of TiO_2 and its associated issues should be eliminated. However, the mechanism for this should be investigated in future research.

Organic matter in secondary effluent also competes with target pharmaceuticals during photocatalysis [43]. When the F9/P25 composite sheet was used to degrade raw RO concentrate without crotamiton spiking, approximately 15% of the initial TOC (10.1 mgC/L) was degraded after 24 h of UV irradiation. The TOC concentration in the RO concentrate was 10.1 mgC/L , and the TOC concentration for the 10 mg/L crotamiton solution in ultrapure water was 7.67 mgC/L theoretically. The coexisting organic matter may compete with crotamiton for consumption of the oxidizing agent during photocatalysis by the F9/P25 composite sheet.

Mineralization during photocatalytic degradation was evaluated by plotting TOC/TOC_0 against time at an initial crotamiton concentration of 10 mg/L (Figure 4). The TOC concentration provided by the residual crotamiton was also determined by performing stoichiometric calculations. During the photocatalytic degradation of crotamiton by the F9/P25 composite sheet in both ultrapure water and RO concentrate, the solution TOC did not obviously decrease with the degradation of crotamiton. This result implied that crotamiton was degraded step by step and that the intermediate compounds accumulated at the same time. Kuo et al., investigated the photocatalytic mineralization of methamphetamine in a UVA/ TiO_2 system and found that TOC disappeared more slowly than methamphetamine because the methamphetamine intermediates took some time to be mineralized [44]. A more detailed discussion on the degradation intermediates is given in Section 3.4.

3.3. Adsorption and Photocatalytic Degradation of Crotamiton by the HSZ-385/P25 Composite Sheet

In our previous research, we found that P25 was effective for photocatalytic degradation of crotamiton [31]. The HSZ-385/P25 composite sheet prepared in the present study combines adsorption and photocatalysis processes, which makes it possible to regenerate the adsorbent during treatment.

To clarify the adsorption and degradation performance of crotamiton by the HSZ-385/P25 composite sheet, the mass of crotamiton in the composite sheet ($M_{in \text{ sheet}}$) was determined together with the mass of crotamiton in the aqueous phase ($M_{in \text{ water}}$). The mass of crotamiton in the system

($M_{in\ system}$) was calculated as the sum of the residual mass of crotamiton in both the aqueous phase and in the sheet, which was the mass of undecomposed crotamiton remaining in the system.

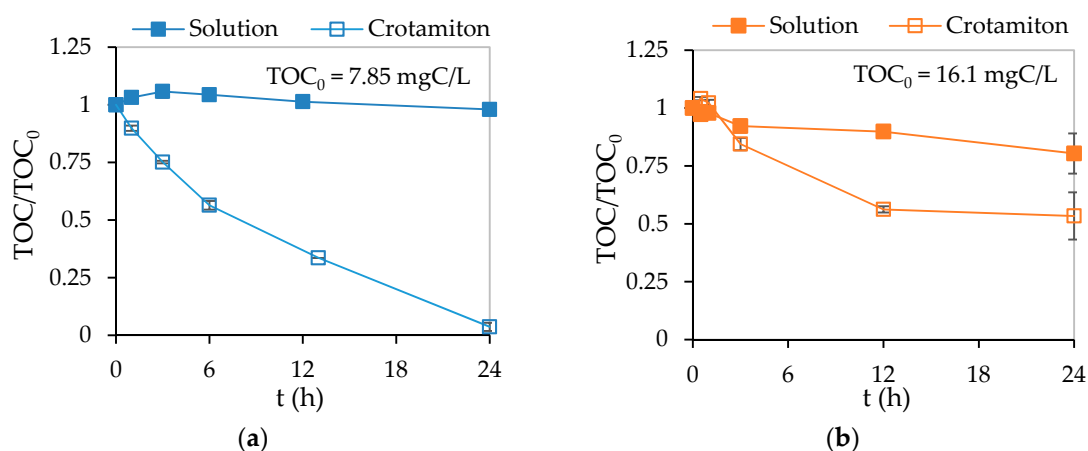


Figure 4. Removal of TOC in the solutions and the TOC derived from the residual crotamiton during the treatment by the F9/P25 composite sheet with ultraviolet irradiation in ultrapure water (a) and RO concentrate (b). Results are means \pm standard deviations ($n = 2$).

The masses of crotamiton in different phases were plotted against time (Figure 5) for solutions with initial crotamiton concentrations of 10 mg/L in ultrapure water (Figure 5a), 10 mg/L in RO concentrate (Figure 5b), and 120 μ g/L in RO concentrate (Figure 5c). Although similar trends were observed for $M_{in\ water}$ in ultrapure water and RO concentrate (Figure 5a,b) with an initial crotamiton concentrations of 10 mg/L, the trends for $M_{in\ sheet}$ were very different. The highest value of $M_{in\ sheet}$ (ca. 0.12 mg) was observed after 3 hr treatment of crotamiton in the ultrapure water, and this then decreased with time (Figure 5a); at most, only 23% of the initial crotamiton was accumulated in the sheet, and all the crotamiton was eventually degraded by photocatalysis.

In removing of crotamiton from the RO concentrate, much more crotamiton (0.34 mg) was accumulated in the composite sheet after 6 h treatment (Figure 5b). After that, the mass of crotamiton in the sheet gradually decreased, and finally 0.25 mg remained in the sheet at 24 hr. The higher removal rate obtained with adsorption compared with photocatalysis led to the accumulation and long retention time of crotamiton in the composite sheet. In the treatment of both RO concentrate and ultrapure water, crotamiton could be effectively removed from the aqueous phase, thus purifying the water. The adsorption process was not greatly affected by the water matrix, but inhibition of photocatalysis resulted in low crotamiton degradation in the RO concentrate when using the HSZ-385/P25 composite sheet.

Removing of crotamiton from the RO concentrate with an initial crotamiton concentration of 120 μ g/L was investigated (Figure 5c). The $M_{in\ sheet}$ values were maintained at a low level throughout the treatment, and the maximum accumulation of crotamiton in the sheet was only 6.7% of the initial crotamiton mass in the aqueous phase. A rapid decrease was observed in $M_{in\ system}$, showing that rapid decomposition of crotamiton occurred with the low initial crotamiton concentration. Inhibition of the degradation process with high initial crotamiton concentrations may be attributed to competition from intermediates produced by crotamiton degradation [37]. Jang et al., found that the target material (trichloroethylene) saturated the composite catalyst surface and reduced photon efficiency, leading to photocatalyst deactivation [45]. Kuo et al., showed that the degradation rates of codeine and methamphetamine increased with increasing initial concentration (100–250 μ g/L) [44,46]. With the initial concentration at microgram per liter levels, the degradation rate may not be limited by the availability of catalytic sites but by contaminant concentration.

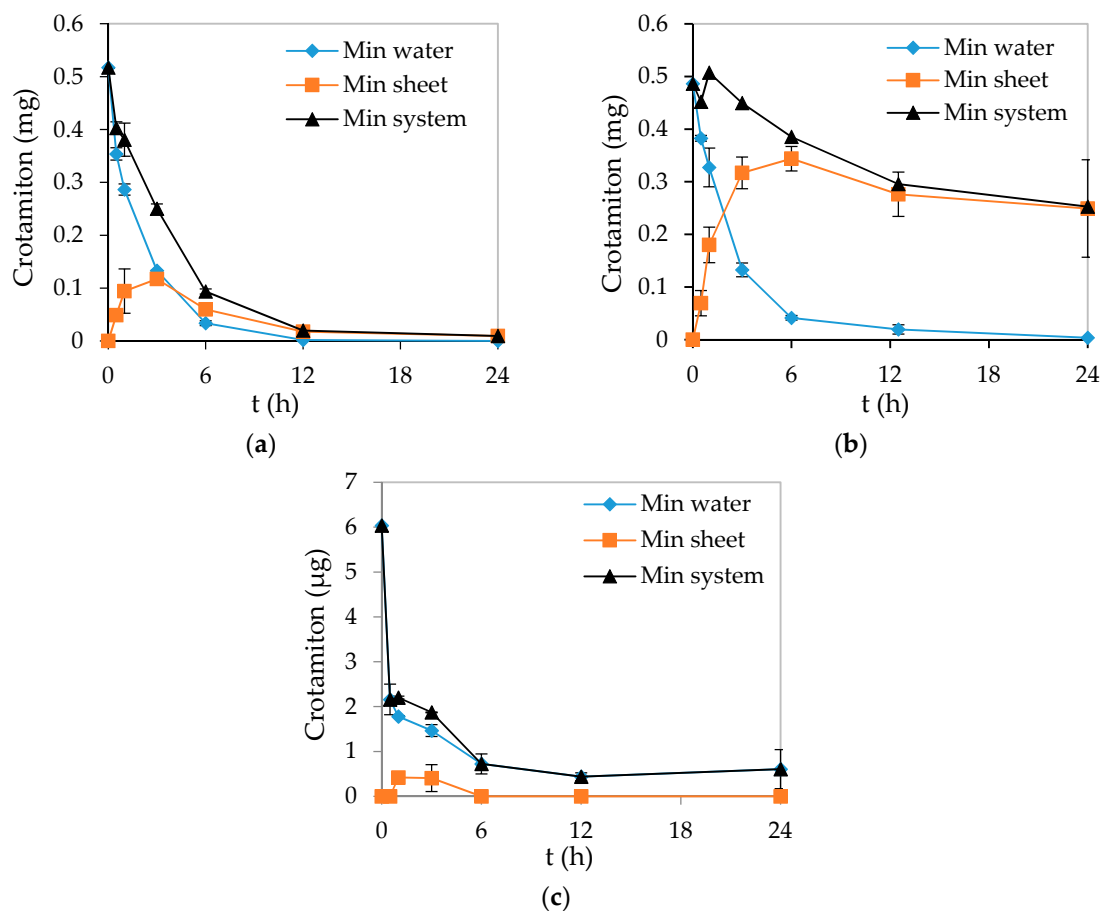


Figure 5. Removal of crotamiton using the HSZ-385/P25 composite sheet with ultraviolet irradiation for solutions of (a) 10 mg/L crotamiton in ultrapure water; (b) 10 mg/L crotamiton in RO concentrate; and (c) 120 µg/L crotamiton in RO concentrate. Results are means \pm standard deviations ($n = 2$).

The TOC/TOC₀ ratios plotted against time in the HSZ-385/P25 composite sheet experiment are shown in Figure 6. With removal of crotamiton in the ultrapure water by the HSZ-385/P25 composite sheet, TOC was gradually removed and the removal efficiency reached up to 84% after 24 hr (Figure 6a), whereas the TOC removal efficiency was stable at ca. 51% after 6 hr of crotamiton treatment in the RO concentrate by the HSZ-385/P25 composite sheet (Figure 6b). The photocatalytic degradation of crotamiton was significantly inhibited by the other components in the RO concentrate. Furthermore, the low TOC removal by individual adsorption or degradation for the organic matter in the original RO concentrate is another important reason. After 24 hr treatment by the HSZ-385/P25 composite sheet, the majority of the crotamiton was removed, which was similar to that in the experiment using the F9/P25 composite sheet. A rather lower TOC/TOC₀ ratio was observed in the treatment using the HSZ-385/P25 composite sheet compared with the F9/P25 composite sheet. It has been assumed that accumulation of degradation intermediates in the experiment using the F9/P25 composite sheet resulted in the high residual TOC concentration in the aqueous phase (Figure 4a). The much lower TOC/TOC₀ in the treatment using the HSZ-385/P25 composite sheet indicated other TOC derived from degradation intermediates in the aqueous phase has been removed because of the function of the HSZ-385 in the composite sheet (Figure 6a). That is to say, not only crotamiton in the solution but also the degradation intermediates of crotamiton were removed by the HSZ-385 in the composite sheet.

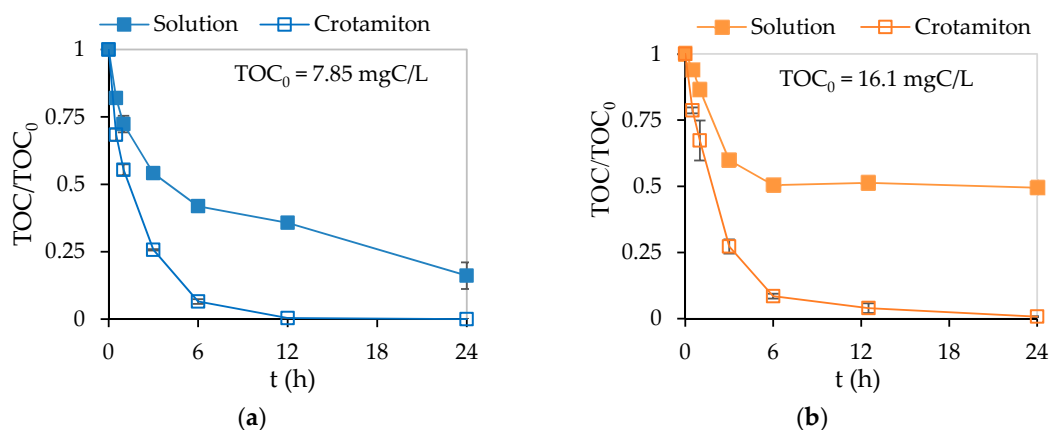


Figure 6. Removal of TOC in the solutions and the TOC derived from the residual crodamiton during the treatment by the HSZ-385/P25 composite sheet with ultraviolet irradiation in ultrapure water (a) and RO concentrate (b). Results are means \pm standard deviations ($n = 2$).

3.4. Behavior of the Degradation Intermediates during Photocatalysis

The degradation intermediates were characterized following the methods described in our previous study [31]. We proposed that P25-catalyzed photodegradation of crodamiton could initially occur via hydroxylation of the aromatic ring, the double bond of the propenyl group, or the ethyl group. These reactions formed intermediates that we labeled as P189, P217, and P219. The peak areas of the intermediates were measured in the selected ion recording mode of LC/MS/MS.

With the degradation of crodamiton, the intermediates gradually accumulated and reached their highest levels in the treatment using the F9/P25 composite sheet (Figure 7). Intermediate P219, which was produced by hydroxylation of the aromatic ring of crodamiton, was the most noticeable degradation intermediate. The peak area of P219 was higher than those for P189 and P217. After 24 hr of treatment, most of the P189 and P217 had disappeared. In contrast, the peak area of P219 was still high after 24 hr of treatment with the F9/P25 composite sheet. This result corresponded well to the high TOC/TOC₀ level revealed in Figure 4a, validating the assumption of the accumulation of degradation intermediates during the treatment by the F9/P25 composite sheet.

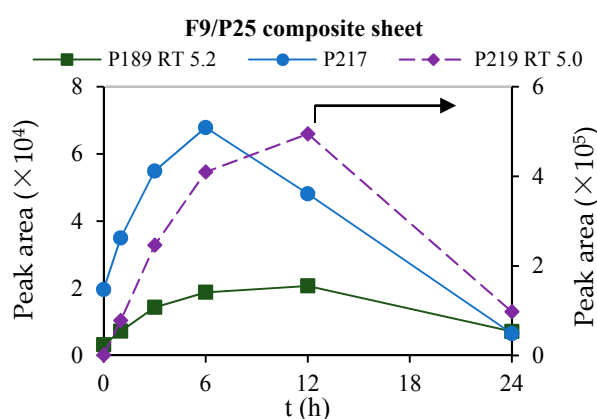


Figure 7. Changes in the peak areas of the major intermediates over time in ultrapure water when crodamiton was photocatalytically degraded using the F9/P25 composite sheet ($C_0 = 10$ mg/L). The squares are P189 (retention time 5.2 min) and the circles are P217. The diamonds with a dashed line are P219 (retention time 5.0 min, secondary y-axis).

Treatment with the HSZ-385/P25 composite sheet (Figure 8) was compared with that using the F9/P25 composite sheet. The peak areas for the three intermediates obtained with the HSZ-385/P25

composite sheet were clearly lower than those obtained with the F9/P25 composite sheet throughout the treatment, especially for intermediate P219. After 24 hr of treatment with the HSZ-385/P25 composite sheet, the majority of all three intermediates had disappeared. The lower peak areas of degradation intermediates as well as the lower TOC/TOC₀ ratios (Figure 6a) confirmed that the HSZ-385/P25 composite sheet captured the degradation intermediates.

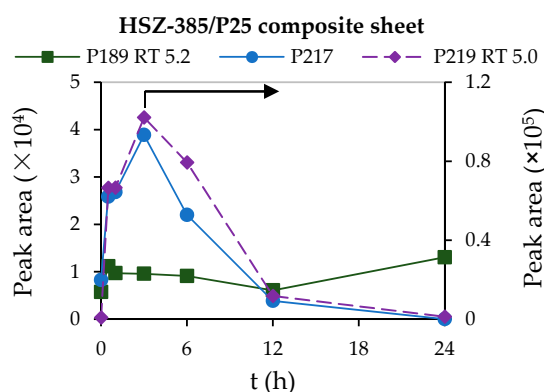


Figure 8. Changes in the peak areas of the major intermediates over time in ultrapure water when crotonamiton was photocatalytically degraded using the HSZ-385/P25 composite sheet ($C_0 = 10$ mg/L). The squares are P189 (retention time 5.2 min) and the circles are P217. The diamonds with a dashed line are P219 (retention time 5.0 min, secondary y -axis).

Moreover, changes in the peak areas for the major intermediates in the HSZ-385/P25 composite sheet were evaluated through desorption treatment for the composite sheet after the adsorption and photocatalysis experiment. The methanol solution with the composite sheet after ultrasonic treatment contained crotonamiton, as well as large amounts of degradation intermediates, retained in the composite sheet (Figure 9). The peak area for P219 was higher in the composite sheet during treatment than that in the aqueous phase when using the HSZ-385/P25 composite sheet shown in Figure 8. Even if the efficiency of desorption of the intermediates from the sheet could not be confirmed without the standard of every detected intermediate, the high peak areas for the intermediates provided direct evidence of the adsorption of intermediates on the composite sheet.

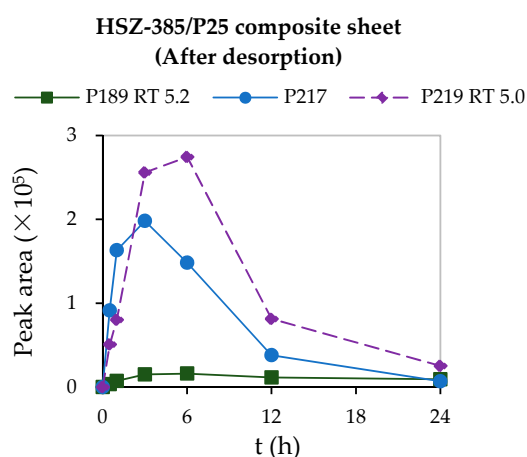


Figure 9. Changes in the areas of the peaks for the major intermediates over time in the HSZ-385/P25 composite sheet after desorption when crotonamiton was photocatalytically degraded using the HSZ-385/P25 composite sheet ($C_0 = 10$ mg/L). The squares are P189 (retention time 5.2 min), the circles are P217, and the diamonds with a dashed line are P219 (retention time 5.0 min).

In conclusion, the HSZ-385/P25 composite sheet is effective not only for removing crotamiton, but also for capturing degradation intermediates produced by photocatalysis. This method mitigates the negative impact of harmful degradation intermediates produced by advanced oxidation processes.

3.5. Cyclic Use of the HSZ-385/P25 Composite Sheet

To effectively apply the HSZ-385/P25 composite sheet to remove crotamiton from RO concentrate in practical treatment processes, it is essential that the composite sheet can remove pollutants even after several cycles of reuse. The efficiency of removing crotamiton from RO concentrate achieved by the HSZ-385/P25 composite sheet after 24 hr ultraviolet irradiation in three circles of reuse were all over 95% (Figure 10). The crotamiton amount in the composite sheet after three cycles of reuse was 0.40 mg, which was ca. 27% of the total amount of three cycles of treated crotamiton ($C_0 = 10$ mg/L, $V = 50$ mL), demonstrating continuous crotamiton photocatalytic degradation. The TOC removal efficiency slightly decreased with an increase in the cycles of reuse. It can be concluded that the HSZ-385/P25 composite sheet is feasible for the cyclic removal of crotamiton in RO concentrate.

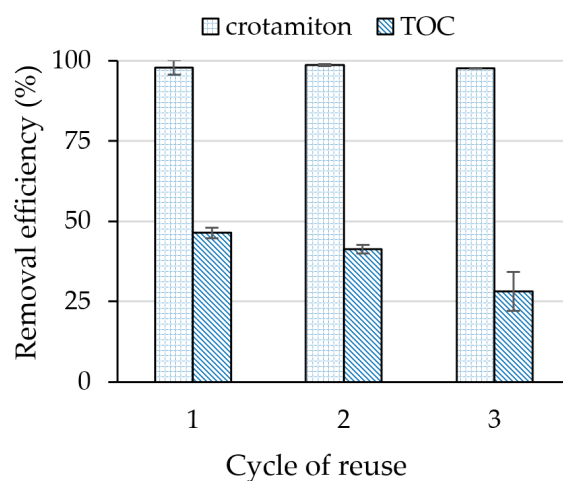


Figure 10. The removal efficiency of crotamiton and TOC in RO concentrate using the HSZ-385/P25 composite sheet after cyclic use. Results are means \pm standard deviations ($n = 2$).

Some other composite materials used as adsorbents and photocatalysts for treating organic pollutants are summarized in Table 2. No previous publications applied composite materials for the treatment of pollutants in RO concentrate. A few cycles of pollutant removal were carried out in studies using TiO_2 -coconut shell powder composite [47], polyacrylic acid-grafted-carboxylic graphene/titanium nanotube composite [48], multi-walled carbon nanotubes/ Fe_3O_4 composites [49], multi-walled carbon nanotube/ TiO_2 composites [50] and nitrogen-doped- TiO_2 /activated carbon composite [51] similar to that in this study. The stability of the photocatalyst and reusability of these materials were confirmed, thus making them promising cost-effective water purification materials.

Except for reusability, some of the composites were designed to promote degradation capability through improving visible light utilization, photon yield, and so on. The presence of MoS_2 in the TiO_2 - MoS_2 -reduced graphene oxide composite worked as a co-catalyst to reduce electron-hole pairs, and improved the photocatalytic performance of TiO_2 for BPA removal [52]. The nitrogen-doped- TiO_2 /activated carbon composite was synthesized to regenerate spent powdered activated carbon using solar photocatalysis for cost-effective application in wastewater treatment [51]. The graphene/ TiO_2 /ZSM-5 composite material showed higher stability, stronger absorption of visible light, and lower band gap value [53].

Table 2. Composite materials synthesized for removing organic pollutants.

Composite	Target Pollutant	Water Matrix	Reference
TiO ₂ -coconut shell powder composite	Carbamazepine, clofibric acid, and triclosan	Ultrapure water	[47]
Polyacrylic acid-grafted-carboxylic graphene/titanium nanotube composite	Enrofloxacin	Distilled water and simulated poultry farm effluent	[48]
Multi-walled carbon nanotubes/Fe ₃ O ₄ composites	Bisphenol A	Doubly-distilled deionized water	[49]
Multi-walled carbon nanotubes/TiO ₂ nanocomposite	Tetracycline	Pharmaceutical wastewater	[50]
Nitrogen-doped-TiO ₂ /activated carbon composite	Bisphenol-A, sulfamethazine, and clofibric acid	Ultrapure water	[51]
TiO ₂ -MoS ₂ -reduced graphene oxide composite	Bisphenol A	Not mentioned	[52]
Graphene/TiO ₂ /ZSM-5 composites	Oxytetracycline	Deionized water	[53]

4. Conclusions

TiO₂/zeolite composite sheets were synthesized and used to remove crotamiton from RO concentrate. Crotamiton is effectively adsorbed by the HSZ-385/P25 composite sheet without obvious inhibition by other components of the RO concentrate. The photocatalytic decomposition of crotamiton in the RO concentrate is significantly inhibited by the water matrix at high initial concentrations of crotamiton, whereas rapid decomposition occurs at low initial concentrations. When the HSZ-385/P25 composite sheet is used with UV irradiation for the removal of crotamiton from RO concentrate, crotamiton is removed by adsorption and photocatalysis. The inhibition of photocatalytic degradation by other components resulted in crotamiton remaining in the composite sheet. The degradation intermediates are captured by the HSZ-385/P25 composite sheet, and this capture provides a way to mitigate the potential negative impact of intermediates from advanced oxidation processes. In addition, the HSZ-385/P25 can continually remove crotamiton from RO concentrate with repeated uses.

Supplementary Materials: The following are available online at <http://www.mdpi.com/2076-3417/7/8/778/s1>, Figure S1: The experimental set-up of the adsorption and photocatalytic degradation of crotamiton using the TiO₂/zeolite composite sheet. The symbol Φ refers to the diameter of the vial; Figure S2: Removal of crotamiton from ultrapure water by adsorption using F9 powder, HSZ-385 powder and the F9/P25 composite sheet ($C_0 = 10$ mg/L, $V = 50$ mL). The dosage for the powder adsorbent was 0.1 g/L. The F9/P25 composite sheet was 2×5.5 cm² and submerged at a depth of 4 cm. The composite sheet contained 4 mg F9/cm².

Acknowledgments: This work was supported by the Japan Society for the Promotion of Science Grants-in-Aid for Scientific Research Grant Number 16H02372. We appreciate the assistance of Suntae Lee with sampling of the RO concentrate. We thank Gabrielle David, from Edanz Group (www.edanzediting.com/ac) and Dennis Murphy of the United Graduate School of Agricultural Sciences, Ehime University, for editing a draft of this manuscript.

Author Contributions: Qun Xiang, Taku Fujiwara and Shuji Fukahori conceived and designed the experiments; Qun Xiang performed the experiments, analyzed the data and wrote the paper; Taku Fujiwara supervised the research; Shuji Fukahori contributed to the preparation and characterization of the composite sheet; Naoyuki Yamashita and Hiroaki Tanaka contributed to the sampling of the RO concentrate and provided advice on the experiments. All authors have read and approved the final manuscript.

Conflicts of Interest: The authors declare no conflict of interest.

References

- Joo, S.H.; Tansel, B. Novel technologies for reverse osmosis concentrate treatment: A review. *J. Environ. Manag.* **2015**, *150*, 322–335. [[CrossRef](#)] [[PubMed](#)]
- Umar, M.; Roddick, F.; Fan, L. Recent advancements in the treatment of municipal wastewater reverse osmosis concentrate—An overview. *Crit. Rev. Environ. Sci. Technol.* **2015**, *45*, 193–248. [[CrossRef](#)]

3. Umar, M.; Roddick, F.; Fan, L. Comparison of coagulation efficiency of aluminium and ferric-based coagulants as pre-treatment for UVC/H₂O₂ treatment of wastewater RO concentrate. *Chem. Eng. J.* **2016**, *284*, 841–849. [[CrossRef](#)]
4. Umar, M.; Roddick, F.; Fan, L. Assessing the potential of a UV-based AOP for treating high-salinity municipal wastewater reverse osmosis concentrate. *Water Sci. Technol.* **2013**, *68*, 1994–1999. [[CrossRef](#)] [[PubMed](#)]
5. Westerhoff, P.; Moon, H.; Minakata, D.; Crittenden, J. Oxidation of organics in retentates from reverse osmosis wastewater reuse facilities. *Water Res.* **2009**, *43*, 3992–3998. [[CrossRef](#)] [[PubMed](#)]
6. Rodriguez-Mozaz, S.; Ricart, M.; Köck-Schulmeyer, M.; Guasch, H.; Bonnineau, C.; Proia, L.; de Alda, M.L.; Sabater, S.; Barceló, D. Pharmaceuticals and pesticides in reclaimed water: Efficiency assessment of a microfiltration-reverse osmosis (MF-RO) pilot plant. *J. Hazard. Mater.* **2015**, *282*, 165–173. [[CrossRef](#)] [[PubMed](#)]
7. Tang, F.; Hu, H.Y.; Wu, Q.Y.; Tang, X.; Sun, Y.X.; Shi, X.L.; Huang, J.J. Effects of chemical agent injections on genotoxicity of wastewater in a microfiltration-reverse osmosis membrane process for wastewater reuse. *J. Hazard. Mater.* **2013**, *260*, 231–237. [[CrossRef](#)] [[PubMed](#)]
8. Subramani, A.; Jacangelo, J.G. Treatment technologies for reverse osmosis concentrate volume minimization: A review. *Sep. Purif. Technol.* **2014**, *122*, 472–489. [[CrossRef](#)]
9. Yang, Y.; Ok, Y.S.; Kim, K.-H.; Kwon, E.E.; Tsang, Y.F. Occurrences and removal of pharmaceuticals and personal care products (PPCPs) in drinking water and water/sewage treatment plants: A review. *Sci. Total Environ.* **2017**, *596–597*, 303–320. [[CrossRef](#)] [[PubMed](#)]
10. Chong, M.N.; Jin, B.; Chow, C.W.K.; Saint, C. Recent developments in photocatalytic water treatment technology: A review. *Water Res.* **2010**, *44*, 2997–3027. [[CrossRef](#)] [[PubMed](#)]
11. Saha, S.; Wang, J.M.; Pal, A. Nano silver impregnation on commercial TiO₂ and a comparative photocatalytic account to degrade malachite green. *Sep. Purif. Technol.* **2012**, *89*, 147–159. [[CrossRef](#)]
12. Salaeh, S.; Perisic, D.J.; Biosic, M.; Kusic, H.; Babic, S.; Stangar, U.L.; Dionysiou, D.D.; Bozic, A.L. Diclofenac removal by simulated solar assisted photocatalysis using TiO₂-based zeolite catalyst; mechanisms, pathways and environmental aspects. *Chem. Eng. J.* **2016**, *304*, 289–302. [[CrossRef](#)]
13. Haynes, V.N.; Ward, J.E.; Russell, B.J.; Agrios, A.G. Photocatalytic effects of titanium dioxide nanoparticles on aquatic organisms—Current knowledge and suggestions for future research. *Aquat. Toxicol.* **2017**, *185*, 138–148. [[CrossRef](#)] [[PubMed](#)]
14. Chen, X.; Fujiwara, T.; Fukahori, S.; Ishigaki, T. Factors affecting the adsorptive removal of bisphenol A in landfill leachate by high silica Y-type zeolite. *Environ. Sci. Pollut. Res.* **2015**, *22*, 2788–2799. [[CrossRef](#)] [[PubMed](#)]
15. Yang, R.T. *Adsorbents: Fundamentals and Applications*; John Wiley & Sons, Inc.: Hoboken, NJ, USA, 2003; ISBN 0471297410.
16. Kyzas, G.Z.; Fu, J.; Lazaridis, N.K.; Bikiaris, D.N.; Matis, K.A. New approaches on the removal of pharmaceuticals from wastewaters with adsorbent materials. *J. Mol. Liq.* **2015**, *209*, 87–93. [[CrossRef](#)]
17. Anastopoulos, I.; Bhatnagar, A.; Hameed, B.H.; Ok, Y.S.; Omirou, M. A review on waste-derived adsorbents from sugar industry for pollutant removal in water and wastewater. *J. Mol. Liq.* **2017**, *240*, 179–188. [[CrossRef](#)]
18. Kyzas, G.Z.; Matis, K.A. Nano-adsorbents for pollutants removal: A review. *J. Mol. Liq.* **2015**, *203*, 159–168. [[CrossRef](#)]
19. Wei, X.; Wang, Y.; Hernández-Maldonado, A.J.; Chen, Z. Guidelines for rational design of high-performance adsorbents: A case study of zeolite adsorbents for emerging pollutants in water. *Green Energy Environ.* **2017**, in press. [[CrossRef](#)]
20. Fukahori, S.; Fujiwara, T.; Funamizu, N.; Matsukawa, K.; Ito, R. Adsorptive removal of sulfonamide antibiotics in livestock urine using the high-silica zeolite HSZ-385. *Water Sci. Technol.* **2013**, *67*, 319–325. [[CrossRef](#)] [[PubMed](#)]
21. Wu, H.; Wu, X.-L.; Wang, Z.-M.; Aoki, H.; Kutsuna, S.; Jimura, K.; Hayashi, S. Anchoring titanium dioxide on carbon spheres for high-performance visible light photocatalysis. *Appl. Catal. B Environ.* **2017**, *207*, 255–266. [[CrossRef](#)]
22. Yap, P.-S.; Cheah, Y.-L.; Srinivasan, M.; Lim, T.-T. Bimodal N-doped P25-TiO₂/AC composite: Preparation, characterization, physical stability, and synergistic adsorptive-solar photocatalytic removal of sulfamethazine. *Appl. Catal. A Gen.* **2012**, *427–428*, 125–136. [[CrossRef](#)]

23. Fukahori, S.; Fujiwara, T. Modeling of sulfonamide antibiotic removal by TiO₂/high-silica zeolite HSZ-385 composite. *J. Hazard. Mater.* **2014**, *272*, 1–9. [[CrossRef](#)] [[PubMed](#)]
24. Li, M.; Lu, B.; Ke, Q.F.; Guo, Y.J.; Guo, Y.P. Synergetic effect between adsorption and photodegradation on nanostructured TiO₂/activated carbon fiber felt porous composites for toluene removal. *J. Hazard. Mater.* **2017**, *333*, 88–98. [[CrossRef](#)] [[PubMed](#)]
25. Fukahori, S.; Ichiura, H.; Kitaoka, T.; Tanaka, H. Photocatalytic decomposition of bisphenol A in water using composite TiO₂-zeolite sheets prepared by a papermaking technique. *Environ. Sci. Technol.* **2003**, *37*, 1048–1051. [[CrossRef](#)] [[PubMed](#)]
26. Fukahori, S.; Ichiura, H.; Kitaoka, T.; Tanaka, H. Capturing of bisphenol A photodecomposition intermediates by composite TiO₂-zeolite sheets. *Appl. Catal. B Environ.* **2003**, *46*, 453–462. [[CrossRef](#)]
27. Nakada, N.; Tanishima, T.; Shinohara, H.; Kiri, K.; Takada, H. Pharmaceutical chemicals and endocrine disrupters in municipal wastewater in Tokyo and their removal during activated sludge treatment. *Water Res.* **2006**, *40*, 3297–3303. [[CrossRef](#)] [[PubMed](#)]
28. Nakada, N.; Yasojima, M.; Okayasu, Y.; Komori, K.; Suzuki, Y. Mass balance analysis of triclosan, diethyltoluamide, crotamiton and carbamazepine in sewage treatment plants. *Water Sci. Technol.* **2010**, *61*, 1739–1747. [[CrossRef](#)] [[PubMed](#)]
29. Tamura, I.; Yasuda, Y.; Kagota, K.; Yoneda, S.; Nakada, N. Ecotoxicology and environmental safety contribution of pharmaceuticals and personal care products (PPCPs) to whole toxicity of water samples collected in effluent-dominated urban streams. *Ecotoxicol. Environ. Saf.* **2017**, *144*, 338–350. [[CrossRef](#)] [[PubMed](#)]
30. Japanese Industrial Standards Committee. Pulps-Preparation of Laboratory Sheets for Physical Testing-Conventional Sheet-Former Method, JIS P8222: 2015. Available online: <http://www.jisc.go.jp/app/jis/general/GnrJISSearch.html> (accessed on 26 July 2017).
31. Fukahori, S.; Fujiwara, T.; Ito, R.; Funamizu, N. Photocatalytic decomposition of crotamiton over aqueous TiO₂ suspensions: Determination of intermediates and the reaction pathway. *Chemosphere* **2012**, *89*, 213–220. [[CrossRef](#)] [[PubMed](#)]
32. Bui, T.X.; Choi, H. Influence of ionic strength, anions, cations, and natural organic matter on the adsorption of pharmaceuticals to silica. *Chemosphere* **2010**, *80*, 681–686. [[CrossRef](#)] [[PubMed](#)]
33. Umar, M.; Roddick, F.; Fan, L. Effect of coagulation on treatment of municipal wastewater reverse osmosis concentrate by UVC/H₂O₂. *J. Hazard. Mater.* **2014**, *266*, 10–18. [[CrossRef](#)] [[PubMed](#)]
34. Fukahori, S.; Fujiwara, T.; Ito, R.; Funamizu, N. pH-Dependent adsorption of sulfa drugs on high silica zeolite: Modeling and kinetic study. *Desalination* **2011**, *275*, 237–242. [[CrossRef](#)]
35. Egerton, T. UV-absorption—The primary process in photocatalysis and some practical consequences. *Molecules* **2014**, *19*, 18192–18214. [[CrossRef](#)] [[PubMed](#)]
36. Tsydenova, O.; Batoev, V.; Batoeva, A. Solar-enhanced advanced oxidation processes for water treatment: Simultaneous removal of pathogens and chemical pollutants. *Int. J. Environ. Res. Public Health* **2015**, *12*, 9542–9561. [[CrossRef](#)] [[PubMed](#)]
37. Tokumura, M.; Sugawara, A.; Raknuzzaman, M.; Habibullah-Al-Mamun, M.; Masunaga, S. Comprehensive study on effects of water matrices on removal of pharmaceuticals by three different kinds of advanced oxidation processes. *Chemosphere* **2016**, *159*, 317–325. [[CrossRef](#)] [[PubMed](#)]
38. Kudlek, E.; Dudziak, M.; Bohdziewicz, J. Influence of inorganic ions and organic substances on the degradation of pharmaceutical compound in water matrix. *Water* **2016**, *8*, 532. [[CrossRef](#)]
39. Zhou, T.; Lim, T.T.; Chin, S.S.; Fane, A.G. Treatment of organics in reverse osmosis concentrate from a municipal wastewater reclamation plant: Feasibility test of advanced oxidation processes with/without pretreatment. *Chem. Eng. J.* **2011**, *166*, 932–939. [[CrossRef](#)]
40. Burns, R.A.; Crittenden, J.C.; Hand, D.W.; Selzer, V.H.; Sutter, L.L.; Salman, S.R. Effect of inorganic ions in heterogeneous photocatalysis of TCE. *J. Environ. Eng.* **1999**, *125*, 77–85. [[CrossRef](#)]
41. Rioja, N.; Benguria, P.; Peñas, F.J.; Zorita, S. Competitive removal of pharmaceuticals from environmental waters by adsorption and photocatalytic degradation. *Environ. Sci. Pollut. Res.* **2014**, *21*, 11168–11177. [[CrossRef](#)] [[PubMed](#)]
42. Song, L.; Zhu, B.; Gray, S.; Duke, M.; Muthukumar, S. Hybrid processes combining photocatalysis and ceramic membrane filtration for degradation of humic acids in saline water. *Membranes* **2016**, *6*. [[CrossRef](#)] [[PubMed](#)]

43. Ito, M.; Fukahori, S.; Fujiwara, T. Adsorptive removal and photocatalytic decomposition of sulfamethazine in secondary effluent using TiO₂-zeolite composites. *Environ. Sci. Pollut. Res.* **2014**, *21*, 834–842. [[CrossRef](#)] [[PubMed](#)]
44. Kuo, C.-S.; Lin, C.-F.; Hong, P.-K.A. Photocatalytic degradation of methamphetamine by UV/TiO₂-Kinetics, intermediates, and products. *Water Res.* **2015**, *74*, 1–9. [[CrossRef](#)] [[PubMed](#)]
45. Jang, D.; Ahn, C.; Choi, J.; Kim, J.; Kim, J.; Joo, J. Enhanced removal of trichloroethylene in water using nano-ZnO/polybutadiene rubber composites. *Catalysts* **2016**, *6*, 152. [[CrossRef](#)]
46. Kuo, C.S.; Lin, C.F.; Hong, P.K.A. Photocatalytic mineralization of codeine by UV-A/TiO₂-Kinetics, intermediates, and pathways. *J. Hazard. Mater.* **2016**, *301*, 137–144. [[CrossRef](#)] [[PubMed](#)]
47. Khraisheh, M.; Kim, J.; Campos, L.; Al-Muhtaseb, A.H.; Al-Hawari, A.; Al Ghouti, M.; Walker, G.M. Removal of pharmaceutical and personal care products (PPCPs) pollutants from water by novel TiO₂-coconut shell powder (TCNSP) composite. *J. Ind. Eng. Chem.* **2014**, *20*, 979–987. [[CrossRef](#)]
48. Anirudhan, T.S.; Shainy, F.; Christa, J. Synthesis and characterization of polyacrylic acid-grafted-carboxylic graphene/titanium nanotube composite for the effective removal of enrofloxacin from aqueous solutions: Adsorption and photocatalytic degradation studies. *J. Hazard. Mater.* **2017**, *324*, 117–130. [[CrossRef](#)] [[PubMed](#)]
49. Huang, Y.; Xu, W.; Hu, L.; Zeng, J.; He, C.; Tan, X.; He, Z. Combined adsorption and catalytic ozonation for removal of endocrine disrupting compounds over MWCNTs/Fe₃O₄ composites. *Catal. Today* **2017**, in press.
50. Ahmadi, M.; Motlagh, H.R.; Jaafarzadeh, N.; Mostoufi, A.; Saeedi, R.; Barzegar, G.; Jorfi, S. Enhanced photocatalytic degradation of tetracycline and real pharmaceutical wastewater using MWCNT/TiO₂ nano-composite. *J. Environ. Manag.* **2017**, *186*, 55–63. [[CrossRef](#)] [[PubMed](#)]
51. Yap, P.-S.; Lim, T.-T. Solar regeneration of powdered activated carbon impregnated with visible-light responsive photocatalyst: Factors affecting performances and predictive model. *Water Res.* **2012**, *46*, 3054–3064. [[CrossRef](#)] [[PubMed](#)]
52. Luo, L.; Li, J.; Dai, J.; Xia, L.; Barrow, C.J.; Wang, H.; Jegatheesan, J.; Yang, M. Bisphenol A removal on TiO₂-MoS₂-reduced graphene oxide composite by adsorption and photocatalysis. *Process Saf. Environ. Prot.* **2017**, in press.
53. Hu, X.-Y.; Zhou, K.; Chen, B.-Y.; Chang, C.-T. Graphene/TiO₂/ZSM-5 composites synthesized by mixture design were used for photocatalytic degradation of oxytetracycline under visible light: Mechanism and biotoxicity. *Appl. Surf. Sci.* **2016**, *362*, 329–334. [[CrossRef](#)]



© 2017 by the authors. Licensee MDPI, Basel, Switzerland. This article is an open access article distributed under the terms and conditions of the Creative Commons Attribution (CC BY) license (<http://creativecommons.org/licenses/by/4.0/>).